

- REZ, P. (1978). *Electron Diffraction, 1927–1977*, pp. 61–67. London: Institute of Physics.
- SPENCER, J. P. & HUMPHREYS, C. J. (1973). *Scanning Electron Microscopy: Systems and Applications*, pp. 126–131. London: Institute of Physics.
- SPENCER, L. V. (1955). *Phys. Rev.* **98**, 1597–1615.
- TAKAGI, S. (1958a). *J. Phys. Soc. Jpn*, **13**, 278–286.
- TAKAGI, S. (1958b). *J. Phys. Soc. Jpn*, **13**, 287–296.
- WHELAN, M. J. (1965a). *J. Appl. Phys.* **36**, 2099–2103.
- WHELAN, M. J. (1965b). *J. Appl. Phys.* **36**, 2103–2110.
- YAMAMOTO, T., MORI, M. & ISHIDA, Y. (1978). *Philos. Mag.* **38**, 439–461.
- YOSHIOKA, H. (1957). *J. Phys. Soc. Jpn*, **12**, 618–628.

*Acta Cryst.* (1980). **A36**, 134–139

## X-ray Diffraction from Nonstoichiometric Titanium Sulfide Containing Stacking Faults

BY M. ONODA AND I. KAWADA

*National Institute for Researches in Inorganic Materials, Sakura-mura, Niihari-gun, Ibaraki, 300-31, Japan*

(Received 16 June 1979; accepted 22 August 1979)

### Abstract

The layer units appropriate to the analysis of titanium sulfide with stacking faults are considered. The layer units composed of one sulfur layer and one titanium layer are adopted for the structures whose stacking sequences are relatively simple. The layer units composed of two sulfur layers, one fully occupied titanium layer, half of a partly occupied titanium layer and half of another partly occupied titanium layer are adopted in the case of the more complex stacking sequences. The general method for obtaining the diffraction intensity distribution by matrices is modified so as to be suitable for the analysis based on these layer units, and examples of the calculated intensity curves are illustrated.

### Introduction

It is often observed that selective broadening and weakening occurs for reflexions with  $h - k \neq 3n$  ( $hkl$ ; indices on the hexagonal cell of the close-packing layers of sulfur) in the X-ray diffraction pattern of nonstoichiometric titanium sulfide. This broadening and weakening suggests the occurrence of stacking faults. For the analysis of structures with stacking faults, the theoretical intensity distribution formulas were derived by Wilson (1942), Hendricks & Teller (1942), Jagodzinski (1949a,b), Paterson (1952), Kakinoki & Komura (1952, 1954a,b, 1965) and Kakinoki (1965, 1966, 1967). The scattering powers are not the same for all the layers in the case of nonstoichiometric titanium sulfide, so the derivation of the expression available for this system is required.

In this paper we consider the layer units appropriate to the titanium–sulfur system and propose a modified procedure to calculate the intensity distribution by using the matrix method given by Kakinoki & Komura.

### The structures of titanium sulfides

In the range  $\text{TiS–TiS}_2$ , several phases such as  $\text{TiS}$ ,  $\text{Ti}_8\text{S}_9$ ,  $\text{Ti}_4\text{S}_5$ ,  $\text{Ti}_3\text{S}_4$ ,  $\text{Ti}_2\text{S}_3$ ,  $\text{Ti}_5\text{S}_8$  and  $\text{TiS}_2$  have been found (Jeannin, 1962; Wiegers & Jellinek, 1970; Tronc & Huber, 1973). The structures of these phases are all based on close-packing layers of sulfur; hexagonal close packing for  $\text{TiS}$  or  $\text{TiS}_2$ , and more complex stacking sequences of  $h$ -packed sulfur layers and  $c$ -packed sulfur layers for the intermediate phases. Titanium atoms always occupy octahedral holes in the close-packing structure of sulfur. These sites are fully and partly occupied in the alternating titanium layers in the composition range  $\text{TiS}_{1.4}$  to  $\text{TiS}_2$ , which corresponds to the existence range of the phases  $\text{Ti}_2\text{S}_3$ ,  $\text{Ti}_5\text{S}_8$  and  $\text{TiS}_2$ . We will discuss such a range, then three kinds of layers are considered; that is sulfur layers, fully occupied titanium layers and partly occupied titanium layers. They are represented by S, Ti and Ti', respectively. The common feature of stacking is represented by ...STiSTi'STiSTi'S... as shown in Fig. 1. We assume that this common feature of stacking is maintained throughout the faulted structure

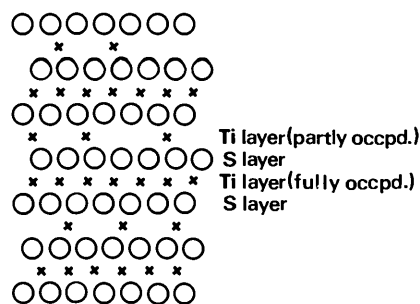


Fig. 1. Schematic drawing of the common stacking features in the range  $\text{TiS}_{1.4}$  to  $\text{TiS}_2$ .



We express the layer form factors for  $V_1, V_2, V_3$  and  $V_4$  as

$$\begin{aligned} V_1 &= L^{1/2}(\xi, \eta) [f_S + f_{Ti} \varepsilon^* \exp(i\pi\zeta)]; \\ V_2 &= L^{1/2}(\xi, \eta) [f_S + y f_{Ti} \varepsilon^* \exp(i\pi\zeta)]; \\ V_3 &= L^{1/2}(\xi, \eta) [f_S + f_{Ti} \varepsilon \exp(i\pi\zeta)]; \\ V_4 &= L^{1/2}(\xi, \eta) [f_S + y f_{Ti} \varepsilon \exp(i\pi\zeta)]; \end{aligned} \quad (4)$$

where  $L(\xi, \eta)$  is the Laue function involving  $\mathbf{a}^*$  and  $\mathbf{b}^*$ ,  $f_S$  and  $f_{Ti}$  are the atomic scattering factors for the S and Ti ions, respectively,  $y$  is the occupancy factor of the partly occupied titanium layer and the composition is represented by  $Ti_{1+y}S_2$ .  $\zeta$  is the coordinate along  $\mathbf{c}^*$ , where  $c^*$  is equal to the reciprocal of the thickness of a layer unit.

The matrix  $\mathbf{P}$  can be rewritten as

$$\mathbf{P} = \begin{pmatrix} \mathbf{0} & \mathbf{P}_1 & \mathbf{P}_2 \\ \mathbf{P}_2 & \mathbf{0} & \mathbf{P}_1 \\ \mathbf{P}_1 & \mathbf{P}_2 & \mathbf{0} \end{pmatrix} \quad (5)$$

and the matrix  $\mathbf{F}$  of existence probabilities of the layer is

$$\mathbf{F} = \frac{1}{3} \begin{pmatrix} \mathbf{W} & \mathbf{0} & \mathbf{0} \\ \mathbf{0} & \mathbf{W} & \mathbf{0} \\ \mathbf{0} & \mathbf{0} & \mathbf{W} \end{pmatrix}, \quad \text{with } \mathbf{W} = \begin{pmatrix} w_1 & 0 & 0 & \dots & 0 \\ 0 & w_2 & 0 & \dots & 0 \\ \vdots & \vdots & \vdots & \ddots & \vdots \\ 0 & 0 & \dots & \dots & w_l \end{pmatrix}, \quad (6)$$

where the orders of the matrices  $\mathbf{P}_1, \mathbf{P}_2$  and  $\mathbf{W}$  are all  $l$ , ( $=4$  in the present case), one third of the order of  $\mathbf{P}$ , and  $\sum_{i=1}^l w_i = 1$ . Then the general method of solution proposed by Kakinoki (1967) can be applied to our case. But as the scattering powers are not the same for all the layer units, minor modification is necessary. The modified procedure is as follows:

*Step 1.* Equation (1) is rewritten as

$$I = \sum_{m=-[N-1]}^{N-1} (N - |m|) J_m \exp(-i2\pi m\zeta), \quad (7)$$

$$J_m = \text{spur } \mathbf{VFP}^m$$

and  $\mathbf{P}_1$  and  $\mathbf{P}_2$  are set from the correct  $\mathbf{P}$ .

*Step 2.* By solving the equation

$$\mathbf{H}(\mathbf{P}_1 + \mathbf{P}_2) = \mathbf{H} \quad \text{with } \mathbf{H} = \begin{pmatrix} w_1 & w_2 & \dots & w_l \\ w_1 & w_2 & \dots & w_l \\ \vdots & \vdots & \ddots & \vdots \\ w_1 & w_2 & \dots & w_l \end{pmatrix}, \quad (8)$$

the existence probability,  $w_i$ , is expressed in terms of elements of the matrix  $\mathbf{P}$ .

*Step 3.*  $J_0, J_1, J_2, \dots$  and  $J_{l-1}$  are calculated by the equation

$$J_m = \text{spur } \mathbf{vW} (\varepsilon \mathbf{P}_1 + \varepsilon^* \mathbf{P}_2)^m, \quad (9)$$

where

$$\mathbf{W} = \begin{pmatrix} \mathbf{v} & \varepsilon^* \mathbf{v} & \varepsilon \mathbf{v} \\ \varepsilon \mathbf{v} & \mathbf{v} & \varepsilon^* \mathbf{v} \\ \varepsilon^* \mathbf{v} & \varepsilon \mathbf{v} & \mathbf{v} \end{pmatrix}$$

$$\text{and } \mathbf{v} = \begin{pmatrix} V_1^* V_1 & V_1^* V_2 & \dots & V_1^* V_l \\ V_2^* V_1 & V_2^* V_2 & \dots & V_2^* V_l \\ \vdots & \vdots & \ddots & \vdots \\ V_l^* V_1 & V_l^* V_2 & \dots & V_l^* V_l \end{pmatrix}$$

*Step 4.*  $a_0, a_1, a_2, \dots$  and  $a_l$  are obtained from the characteristic equation  $F(x)$ ,

$$\begin{aligned} F(x) &= \det(x\mathbf{I} - \varepsilon \mathbf{P}_1 - \varepsilon^* \mathbf{P}_2) \\ &= \sum_{n=0}^l a_n x^{l-n} = 0, \end{aligned} \quad (10)$$

where  $\mathbf{I}$  is a unit matrix of order  $l$ .

*Step 5.*  $J_m$  and  $a_n$  are substituted into the formula for the diffuse intensity term:

$$\begin{aligned} D(\zeta) &= I / [L(\xi, \eta) N] \\ &= \sum_{\nu=0}^{l-1} \left\{ \left[ \sum_{p=0}^{\nu} a_{\nu-p} J_p / L(\xi, \eta) \right] \right. \\ &\quad \times \exp(-i2\pi\nu\zeta) \left. \right\} \left[ \sum_{\nu=0}^l a_{\nu} \exp(-i2\pi\nu\zeta) \right]^{-1} \\ &\quad + \text{conj} - J_0 / L(\xi, \eta). \end{aligned} \quad (11)$$

The principles of the steps are comprehensible in a similar manner to that described by Kakinoki & Komura (1965) and Kakinoki (1966, 1967). Following these procedures the diffuse intensity curve of the model of a  $\mathbf{P}$  table shown in Table 1 was calculated. We obtained

$$\mathbf{P}_1 = \begin{pmatrix} & & & \\ & 1 - \alpha & & \alpha \\ 1 - \alpha & & & \alpha \\ & \alpha & & 1 - \alpha \\ \alpha & & 1 - \alpha & \end{pmatrix},$$

$$\mathbf{P}_2 = \begin{pmatrix} & & & \\ & & & \\ \alpha & & & \\ & 1 - \alpha & & \\ & & & \end{pmatrix}$$

and  $w_1 = w_2 = w_3 = w_4 = 0.25$ .  $J_m$  and  $a_n$  were calculated and substituted into (11) using a computer (FACOM 230-35). The atomic scattering factors,  $f_S$

and  $f_{\text{Ti}}$ , which are contained in the expression of the layer form factor, equation (4), were approximated by the quadratic function of  $\zeta$  by assuming the cell constants of  $\text{Ti}_2\text{S}_3$  and the wavelength of  $\text{Cu } K\alpha$ . The intensity curves along the  $10.\zeta$  reciprocal-lattice line calculated for a fault probability  $\alpha$  varying from 0.1 to 0.9 stepwise are illustrated in Fig. 4 for  $y = 0.33$ .

**Layer unit composed of two sulfur layers, one fully occupied titanium layer, half of a partly occupied titanium layer and half of another partly occupied titanium layer**

Next we consider the structure which has a larger stacking period such as  $\text{Ti}_5\text{S}_8$ , which was called  $12R$  by Tronc & Huber (1973) by analogy with the polytype of  $\text{CdI}_2$ . It is convenient to adopt layer units which are easily related to the customary expression of the stacking sequence such as  $hhcchcc\dots$ . We imagine that a partly occupied titanium layer has been cut in two perpendicularly to the  $c$  axis, and then we try to adopt layer units composed of two sulfur layers, one fully occupied titanium layer, half of a partly occupied titanium layer and half of another partly occupied titanium layer, as illustrated in Fig. 5. There are 24 kinds of layers:  $1A, 1B, 1C, 2A, 2B, 2C, \dots, 8A, 8B$  and  $8C$ . The layer form factors are expressed by

$$\begin{aligned} V_{1A} &= V_1, & V_{1B} &= V_1 \varepsilon^*, & V_{1C} &= V_1 \varepsilon; \\ V_{2A} &= V_2, & V_{2B} &= V_2 \varepsilon^*, & V_{2C} &= V_2 \varepsilon; \\ &\vdots & &\vdots & &\vdots \\ V_{8A} &= V_8, & V_{8B} &= V_8 \varepsilon^*, & V_{8C} &= V_8 \varepsilon. \end{aligned} \quad (12)$$

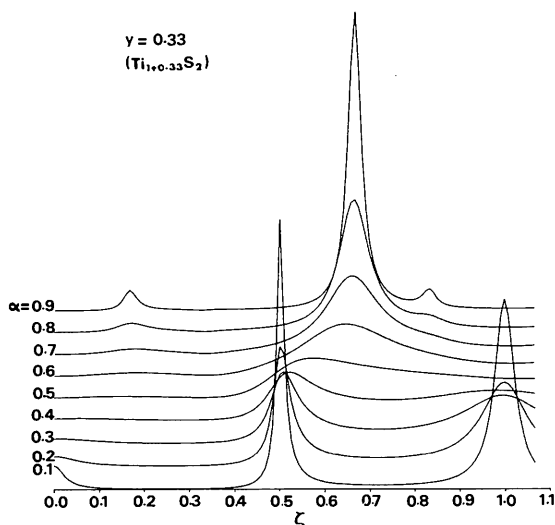


Fig. 4. Intensity curves along the  $10.\zeta$  line calculated for the model of Table 1.

The layer form factors of  $V_1, V_2, \dots$  and  $V_8$  are given by

$$\begin{aligned} V_1 &= L^{1/2}(\xi, \eta) \{ (yf_{\text{Ti}}/2) [1 + \exp(-i2\pi\zeta)] \\ &\quad + f_s \varepsilon \exp(-i\pi\zeta/2) + f_{\text{Ti}} \exp(-i\pi\zeta) \\ &\quad + f_s \varepsilon^* \exp(-i3\pi\zeta/2) \} \\ V_2 &= L^{1/2}(\xi, \eta) \{ (yf_{\text{Ti}}/2) [\varepsilon^* + \exp(-i2\pi\zeta)] \\ &\quad + f_s \exp(-i\pi\zeta/2) + f_{\text{Ti}} \varepsilon \exp(-i\pi\zeta) \\ &\quad + f_s \varepsilon^* \exp(-i3\pi\zeta/2) \} \\ V_3 &= L^{1/2}(\xi, \eta) \{ (yf_{\text{Ti}}/2) [\varepsilon + \exp(-i2\pi\zeta)] \\ &\quad + f_s \exp(-i\pi\zeta/2) + f_{\text{Ti}} \varepsilon \exp(-i\pi\zeta) \\ &\quad + f_s \varepsilon^* \exp(-i3\pi\zeta/2) \} \\ V_4 &= L^{1/2}(\xi, \eta) \{ (yf_{\text{Ti}}/2) [\varepsilon^* + \exp(-i2\pi\zeta)] \\ &\quad + f_s \varepsilon \exp(-i\pi\zeta/2) + f_{\text{Ti}} \exp(-i\pi\zeta) \\ &\quad + f_s \varepsilon^* \exp(-i3\pi\zeta/2) \} \\ V_5 &= L^{1/2}(\xi, \eta) \{ (yf_{\text{Ti}}/2) [\varepsilon + \exp(-i2\pi\zeta)] \\ &\quad + f_s \varepsilon^* \exp(-i\pi\zeta/2) + f_{\text{Ti}} \exp(-i\pi\zeta) \\ &\quad + f_s \varepsilon \exp(-i3\pi\zeta/2) \} \\ V_6 &= L^{1/2}(\xi, \eta) \{ (yf_{\text{Ti}}/2) [\varepsilon^* + \exp(-i2\pi\zeta)] \\ &\quad + f_s \exp(-i\pi\zeta/2) + f_{\text{Ti}} \varepsilon^* \exp(-i\pi\zeta) \\ &\quad + f_s \varepsilon \exp(-i3\pi\zeta/2) \} \\ V_7 &= L^{1/2}(\xi, \eta) \{ (yf_{\text{Ti}}/2) [\varepsilon + \exp(-i2\pi\zeta)] \\ &\quad + f_s \exp(-i\pi\zeta/2) + f_{\text{Ti}} \varepsilon^* \exp(-i\pi\zeta) \\ &\quad + f_s \varepsilon \exp(-i3\pi\zeta/2) \} \\ V_8 &= L^{1/2}(\xi, \eta) \{ (yf_{\text{Ti}}/2) [1 + \exp(-i2\pi\zeta)] \\ &\quad + f_s \varepsilon^* \exp(-i\pi\zeta/2) + f_{\text{Ti}} \exp(-i\pi\zeta) \\ &\quad + f_s \varepsilon \exp(-i3\pi\zeta/2) \}. \end{aligned} \quad (13)$$

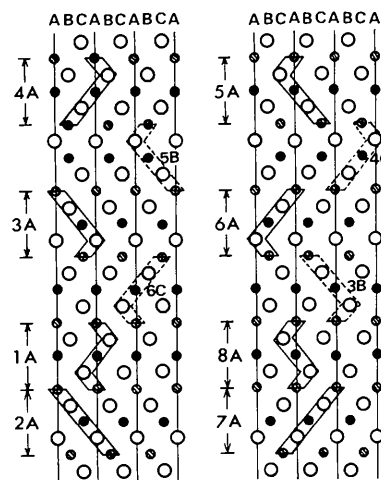


Fig. 5. Imaginary stacking model for illustrating layer units containing two sulfur layers.  $\circ$  sulfur site;  $\bullet$  fully occupied titanium site;  $\otimes$  partly occupied titanium site.

The constitutions of the layer units, 1A, 2A, 3A, ... and 8A, are respectively represented by  $a^+(h-h)a^+$ ,  $b^+(c+c)a^+$ ,  $c^-(h+c)a^+$ ,  $b^-(c-h)a^+$ ,  $c^+(c+h)a^-$ ,  $b^+(h-c)a^-$ ,  $c^-(c-c)a^-$  and  $a^-(h+h)a^-$ .  $h$  and  $c$  represent the packing character of a sulfur layer, that is a layer is denoted by  $h$  if the two neighboring sulfur layers are in the same position (e.g. both A) or by  $c$  if they are in different positions (e.g. A and C). Sandwiched + or - represents the fully occupied titanium layer situated between the positive or negative pair of sulfur layers, where the terms positive and negative are used as in Patterson & Kasper (1967).  $a^+$ ,  $b^+$  and  $c^+$  represent the site of half of the partly occupied titanium layer inserted between the positive pair of the sulfur layers, and  $a^-$ ,  $b^-$  and  $c^-$  represent that inserted between the negative pair. The representations for  $nB$  and  $nC$  result from those for  $nA$  ( $n = 1, 2, \dots, 7, 8$ ) with the cyclic permutation  $a \rightarrow b \rightarrow c$ ,  $b \rightarrow c \rightarrow a$  and  $c \rightarrow a \rightarrow b$ .

As an example, a **P** table based on a model, in which, for example, 1A is followed only by 2C or 5B, is shown in Table 2. In common with the **P** table based on the layer units described above, the values of the elements except those enclosed with thin lines in Table 2 are all zero because, for example,  $a^+$  must be followed by  $a^+$  in order to compose a complete layer. **P** is no longer rewritten in the form of (5) but as

$$\mathbf{P} = \begin{pmatrix} \mathbf{P}_0 & \mathbf{P}_1 & \mathbf{P}_2 \\ \mathbf{P}_2 & \mathbf{P}_0 & \mathbf{P}_1 \\ \mathbf{P}_1 & \mathbf{P}_2 & \mathbf{P}_0 \end{pmatrix}. \quad (14)$$

Then the general method of solution should be further modified. The following equations should be substituted for (8), (9) and (10), respectively:

$$\mathbf{H}(\mathbf{P}_0 + \mathbf{P}_1 + \mathbf{P}_2) = \mathbf{H}; \quad (15)$$

$$J_m = \text{spur } \mathbf{vW}(\mathbf{P}_0 + \varepsilon\mathbf{P}_1 + \varepsilon^*\mathbf{P}_2)^m; \quad (16)$$

$$F(x) = \det(x\mathbf{I} - \mathbf{P}_0 - \varepsilon\mathbf{P}_1 - \varepsilon^*\mathbf{P}_2) = \sum_{n=0}^l a_n x^{l-n} = 0. \quad (17)$$

Table 2. **P** table based on the layer units illustrated in Fig. 5

	1A	2A	3A	4A	5A	6A	7A	8A	1B	2B	3B	4B	5B	6B	7B	8B	1C	2C	3C	4C	5C	6C	7C	8C	
$c^+(h)h^+$	1A																								
$b^+(c)cd^+$	2A	$1-\alpha$																							
$c^-(h)cd^+$	3A	$1-\alpha$																							
$b^-(c)h^+$	4A																								
$c^+(c)h^+$	5A																								
$b^+(h)cd^+$	6A																								
$c^-(c)cd^+$	7A																								
$a^-(h)h^+$	8A																								
$b^-(h)h^+$	1B																								
$c^-(c)cd^+$	2B																								
$a^-(h)cd^+$	3B																								
$c^-(c)h^+$	4B																								
$a^-(c)h^+$	5B																								
$c^-(h)cd^+$	6B																								
$a^-(c)cd^+$	7B																								
$b^-(h)h^+$	8B																								
$c^-(h)h^+$	1C																								
$a^-(c)cd^+$	2C																								
$b^-(h)cd^+$	3C																								
$a^-(c)cd^+$	4C																								
$b^-(h)cd^+$	5C																								
$a^-(h)cd^+$	6C																								
$b^-(c)cd^+$	7C																								
$c^-(h)h^+$	8C																								

In the case of Table 2, the matrices  $(\mathbf{P}_0 + \mathbf{P}_1 + \mathbf{P}_2)$  and  $(\mathbf{P}_0 + \varepsilon\mathbf{P}_1 + \varepsilon^*\mathbf{P}_2)$  are set as shown in Table 3 from the **P** table. The existence probabilities are obtained as

$$w_1 = w_2 = w_7 = w_8 = (1 - \alpha)/4, \quad (18)$$

$$w_3 = w_4 = w_5 = w_6 = \alpha/4,$$

by solving (15). We calculated the diffuse intensity curves as shown in Fig. 6 according to the modified general method of solution by using (13). When the

Table 3. (a)  $(\mathbf{P}_0 + \mathbf{P}_1 + \mathbf{P}_2)$  table and (b)  $(\mathbf{P}_0 + \varepsilon\mathbf{P}_1 + \varepsilon^*\mathbf{P}_2)$  table set from the **P** table shown in Table 2

(a)	1	2	3	4	5	6	7	8
1		$1-\alpha$			$\alpha$			
2	$1-\alpha$					$\alpha$		
3	$1-\alpha$					$\alpha$		
4		$1-\alpha$			$\alpha$			
5				$\alpha$				$1-\alpha$
6			$\alpha$					$1-\alpha$
7			$\alpha$					$1-\alpha$
8				$\alpha$			$1-\alpha$	

(b)	1	2	3	4	5	6	7	8
1		$\varepsilon^*(1-\alpha)$			$\varepsilon\alpha$			
2	$1-\alpha$					$\varepsilon^*\alpha$		
3	$1-\alpha$					$\varepsilon^*\alpha$		
4		$\varepsilon^*(1-\alpha)$			$\varepsilon\alpha$			
5				$\varepsilon^*\alpha$				$\varepsilon(1-\alpha)$
6			$\varepsilon\alpha$					$1-\alpha$
7			$\varepsilon\alpha$					$1-\alpha$
8				$\varepsilon^*\alpha$			$\varepsilon(1-\alpha)$	

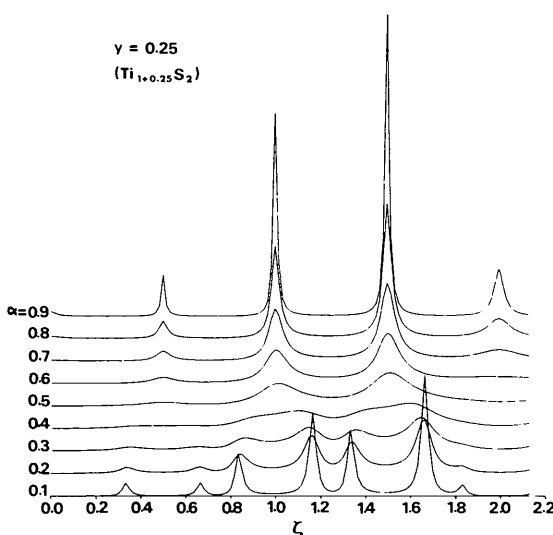


Fig. 6. Intensity curves along the 10.  $\zeta$  line calculated for the model of Table 2.

value of  $\alpha$  is close to zero, the stacking sequences are such as  $a^+(h-h)a^+(c+c)c^+(h-h)c^+(c+c)b^+(h-h)b^+(c+c)a^+ \dots$ , in a concise representation  $hhcchhcc\dots$ , that is the  $Ti_5S_8$  structure. When the value of  $\alpha$  is close to unity, the stacking sequences are such as  $a^+(c+h)b^-(c-h)a^+(c+h)b^-(c-h)a^+ \dots$ , in a concise representation  $chch\dots$ , that is the  $Ti_2S_3$  structure. For the intermediate value of  $\alpha$ , the intensity distribution of the faulted  $Ti_5S_8$  structure where the  $(c+c)$  layer is replaced by the  $(c+h)$  layer at the probability of  $\alpha$  and so forth is displayed among the reciprocal-lattice line  $10.\zeta$  in Fig. 6. The value of  $\zeta$  is twice as large as that shown in Fig. 4, because  $c^*$  is taken as equal to the reciprocal of the thickness of a layer unit.

The contents of the P table based on the layer units described above are easily related to the stacking sequences which are usually expressed by  $c$  and  $h$ . If  $y$  in  $Ti_{1+y}S_2$  approaches zero, the partly occupied titanium layer corresponds to the van der Waals' gap between sulfur-titanium-sulfur sandwiches. In addition, these layer units can be effectively applied to depict the polytype-like phenomena observed by Tronc & Huber (1973). Then the layer units shown in Fig. 5 are convenient for considering the stacking problem in the titanium-sulfur system.

*Acta Cryst.* (1980). **A36**, 139–142

## A Simple Method to Correct for Secondary Extinction in Polarized-Neutron Diffractometry

BY R. CHAKRAVARTHY AND L. MADHAV RAO

*Nuclear Physics Division, Bhabha Atomic Research Centre, Trombay, Bombay 400085, India*

(Received 10 July 1979; accepted 10 September 1979)

### Abstract

In polarized-neutron diffractometry, one often observes a variation of the polarization ratio over the rocking curve. This paper outlines a simple method which uses this interesting feature to estimate quantitatively the secondary-extinction parameter in the specimen crystal.

### Introduction

In polarized-neutron diffractometry, where the aim is to obtain magnetic form factors or spin-density distributions in magnetic crystals, one has to measure with

### References

- HENDRICKS, S. & TELLER, E. (1942). *J. Chem. Phys.* **10**, 147–167.  
 JAGODZINSKI, H. (1949a). *Acta Cryst.* **2**, 201–207.  
 JAGODZINSKI, H. (1949b). *Acta Cryst.* **2**, 208–214.  
 JEANNIN, Y. (1962). *Ann. Chim. (Paris)*, **7**, 57–83.  
 KAKINOKI, J. (1965). *Nippon Kessho Gakkaishi* (in Japanese), **7**, 66–97.  
 KAKINOKI, J. (1966). *Nippon Kessho Gakkaishi* (in Japanese), **8**, 15–33.  
 KAKINOKI, J. (1967). *Acta Cryst.* **23**, 875–885.  
 KAKINOKI, J. & KOMURA, Y. (1952). *J. Phys. Soc. Jpn*, **7**, 30–35.  
 KAKINOKI, J. & KOMURA, Y. (1954a). *J. Phys. Soc. Jpn*, **9**, 169–176.  
 KAKINOKI, J. & KOMURA, Y. (1954b). *J. Phys. Soc. Jpn*, **9**, 177–183.  
 KAKINOKI, J. & KOMURA, Y. (1965). *Acta Cryst.* **19**, 137–147.  
 PATERSON, M. S. (1952). *J. Appl. Phys.* **23**, 805–811.  
 PATTERSON, A. L. & KASPER, J. S. (1967). *International Tables for X-ray Crystallography*, Vol. II, pp. 342–354. Birmingham: Kynoch Press.  
 TRONC, E. & HUBER, M. (1973). *J. Phys. Chem. Solids*, **34**, 2045–2058.  
 WIEGERS, G. A. & JELLINEK, F. (1970). *J. Solid State Chem.* **1**, 519–525.  
 WILSON, A. J. C. (1942). *Proc. R. Soc. London Ser. A*, **180**, 277–285.

considerable precision the magnetic structure factor,  $M$ . In these experiments,  $M$  is arranged to interfere either constructively or destructively with the nuclear structure factor  $N$  (see, for example, Nathans & Pickart, 1963). Thus, for the two states of incident neutron polarization, the peak Bragg intensities are  $I^+ \propto (N + M)^2$  and  $I^- \propto (N - M)^2$ , respectively. The measurement of the ratio of these two peak intensities, called the polarization ratio  $R$ , leads to a determination of  $M/N$ . Provided one knows accurately the nuclear structure factor, the magnetic structure factor can be directly obtained from the measurement of  $R$ . However, in the presence of extinction, the true polarization ratio  $R_0$  will differ from the observed one  $R_{\text{obs}}$  as follows.  $R_{\text{obs}} = R_0 y^+ / y^-$ , where  $y^\pm$  are the extinction